XIV. PHYSICAL ACOUSTICS*

Prof. U. Ingard	L. W. Dean III	M. D. Mintz
Prof. R. D. Fay	P. Gottlieb	M. B. Moffett
Dr. W. W. Lang	G. C. Maling, Jr.	S. K. Oleson
L. C. Bahiana	E. J. Martens, Jr.	H. L. Willke, Jr.

A. INTRODUCTION

For the past few years, research in physical acoustics at M.I.T. has been part of the program of the Acoustics Laboratory, but recently the administration of this research has been transferred to Research Laboratory of Electronics. Since this is our first contribution to the R.L.E. Quarterly Progress Reports, it may be well to describe briefly the scope of our work. In general terms, our research objectives concern the physical problems involved in the generation, propagation, and absorption of sound and vibrations in matter. More specifically, our present research interests include: acoustics of moving media, absorption of sound in metals, electromechanical and magnetomechanical transduction, ultrasonics, and nonlinear acoustics. In this report some of the recent work is described. It should also be mentioned that attempts are being made to generate sound at a frequency of 3×10^9 cps in quartz. Furthermore, we have initiated an investigation of the magnetomechanics of extended systems, together with a study of magnetomechanical and electrical analogs of magnetohydrodynamic systems.

U. Ingard

B. NOISE GENERATION BY INTERACTING AIR JETS

In experiments that have been described elsewhere (1, 2), it was observed that the excess noise produced as a result of the interaction, or mixing, of two small air jets is considerably greater than the noise produced by the individual jets. In principle, it is convenient in the study of the noise generated by flow to differentiate between the noise produced by the turbulent fluctuations alone and the noise produced by the interaction of these fluctuations with the mean flow in regions where mean flow gradients exist. In practice, it is difficult to separate these two contributions. In the experiment on interacting jets, however, the second effect seems to be predominant, and experiments of this kind are therefore of interest for learning about the characteristics of the "shear-generated noise."

Figure XIV-1 shows the sound power caused by the interaction of two air jets in the same plane which intersect between angles of 0° and 180°. This acoustic power is expressed in decibels relative to the total power of the two noninteracting individual jets. The diameter of the jets is 5/8 inch, and the flow velocities 535 feet per second. The distance from the jet exits to the center of the interaction region is kept constant.

If the interaction noise is mainly caused by the effect of the mean gradients, as discussed in the first paragraph, it is possible to explain the results obtained by the

*This research was supported in part by the U. S. Navy (Office of Naval Research) under Contract Nonr-1841(42); and in part by the U. S. Air Force (Air Force Cambridge Research Center, Air Research and Development Command) under Contract AF19(604)-2051.

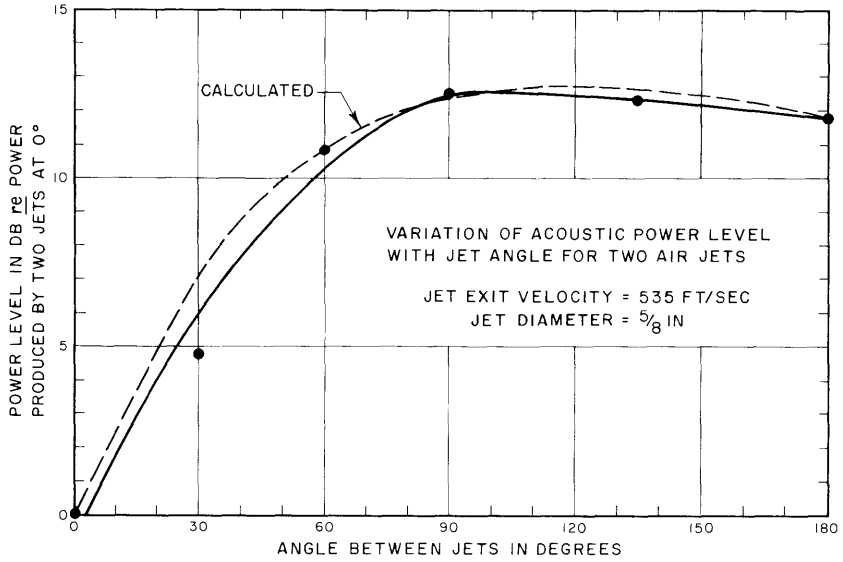

Fig. XIV-1. Interaction level as a function of interaction angle.

following argument: Let us denote the mean flow velocities by the vectors $\underline{V}_2$ and $\underline{V}_1$. At the plane of intersection of the two jets, the gradient in the flow is of the order of $(\underline{V}_1 - \underline{V}_2)/d$, where d is the jet diameter. If the jet velocities have the same magnitude, we obtain

$$|\underline{V}_1| = |\underline{V}_2|, \quad |\underline{V}_1 - \underline{V}_2| = 2|V| \sin\frac{\theta}{2}$$

where θ is the angle between the two jets. The flux of momentum transfer from one jet to another as a result of the turbulent fluctuations of the jets can therefore be set proportional to this velocity gradient and the turbulent velocity fluctuations. From the general theory of the generation of sound by turbulence, the sound generated as a result of the existence of the flow gradient should be proportional to the second power of the flow gradient. Therefore, in this experiment the angular dependence of the interaction noise should be $V^2 \sin^2\frac{\theta}{2} = \frac{1}{2} V^2(1 - \cos\theta)$.

Actually, there is a correction factor that must be introduced to account for the convection of the sound sources, the speed of which can be set approximately equal to $V \cos\theta/2$. The correction factor (3) that applies to flowing quadrupoles is given by the expression $(1 + 1.5\, M^2)/(1 - M^2)^4$. With $M = 0.5 \cos\theta/2$, we find for the interaction noise power

$$P_{int} = \text{constant}\ (1 - \cos\theta)\ \frac{1 + 0.4 \cos^2\frac{\theta}{2}}{\left(1 - 0.25 \cos^2\frac{\theta}{2}\right)^4} \qquad (1)$$

in which the constant is independent of θ but proportional to the mean flow, V^2.

If the acoustic power output of a single jet is denoted by P, the interaction noise level (IL) can be expressed as

$$IL = 10 \log \frac{2P + P_{int}}{2P} = 10 \log \left(1 + \frac{P_{int}}{2P}\right) \tag{2}$$

If we set the constant in Eq. 1 equal to 2KP, where K is a new dimensionless constant, the interaction level becomes

$$IL = 10 \log \left[1 + K(1 - \cos \theta) \frac{1 + 0.4 \cos^2 \frac{\theta}{2}}{\left(1 - 0.25 \cos^2 \frac{\theta}{2}\right)^4}\right] \tag{3}$$

The constant K is chosen to fit the experimental data at $\theta = 90°$, which gives K = 7.5. The angular dependence of the IL, as given by Eq. 3, is then represented by the calculated curve shown in Fig. XIV-1. We see that this curve is in relatively good agreement with the experimental results.

The constant depends on the distance from the jet exit to the interaction region, and the value K = 7.5 corresponds to a distance x = 4.5 jet diameters. However, it would be a simple matter to determine K as a function of x from measurements similar to those described.

It is interesting to investigate the interaction noise when the jets do not lie in the same horizontal plane and, hence, intersect each other only partially, as illustrated in Fig. XIV-2. In the experiments, the vertical distance, d, between the centers of the jets was varied from 0 to 1.25 inches, both up and down. In these preliminary measurements the sound pressure level was measured at only one point outside the interaction region, that is, at approximately 3 feet vertically from the center of the interaction region. The result of these measurements is shown in Fig. XIV-3. The curve is roughly symmetrical, but the center is displaced approximately 1/8 inch from d = 0. This displacement might be caused by a slight asymmetry in the flow speed of one of the jets. The interesting feature of the curve is that the maxima occur on either side of the center position.

As a tentative explanation of the result presented in Fig. XIV-3, we again assume that the interaction noise can be estimated by considering the turbulent fluctuations interacting with the mean flow gradients in the interaction region, as indicated previously. The interaction noise then should be determined by the product of the turbulent fluctuations of one jet at a certain point and the vector difference in the mean flow speed at that point integrated over the interaction region. It can be shown from arguments that include dimensional considerations that the product should have the form $(u)^6 \text{grad}^2 V_{local}$, where u represents the velocity fluctuation.

For interacting jets, let us denote the mean flow speed of the jet at a distance y from the jet by $V = V_o f(\eta, \xi)$, where $\eta = y/d$ and $\xi = x/d$. Here, d is the diameter of

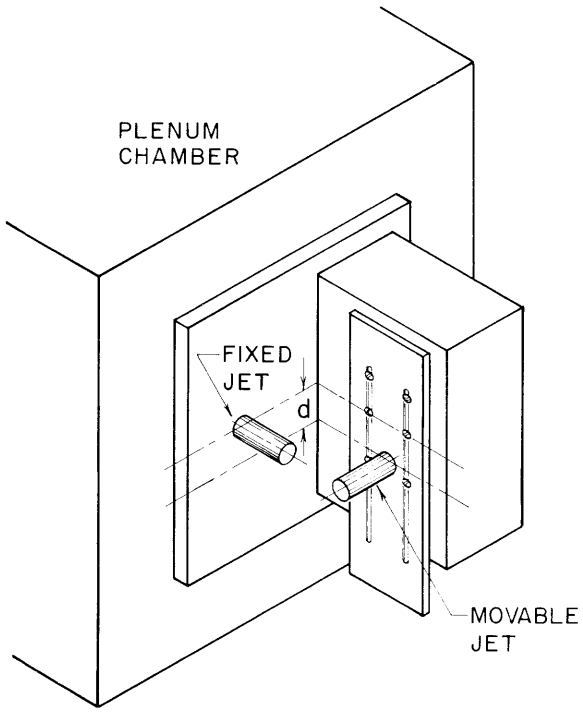

Fig. XIV-2. Experimental arrangement showing orientation of jets.

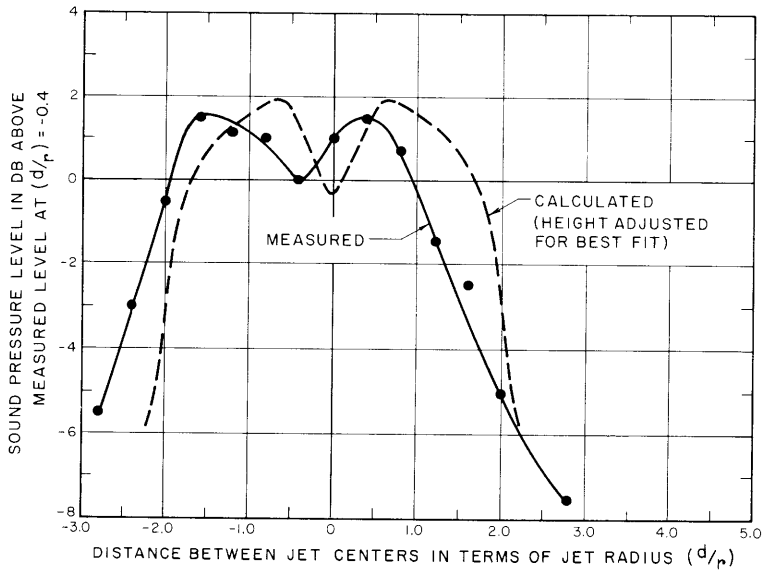

Fig. XIV-3. Sound pressure levels as a function of jet separation.

the jet at the nozzle ($x = 0$), and V_o the velocity of the jet at the center ($y = 0$). Similarly, the fluctuating velocity at the same point is denoted by $u = u_o g(\eta, \xi)$.

The function f can be found from pitot-tube measurements, and g from hot-wire measurements in the jet. An extensive set of such measurements has been reported by Lawrence (4) for geometries and flow speeds that are applicable to the present case. From the mechanism of the interaction noise that has been described, it follows that the power from an element located at a distance y_1 from the center of the first jet and a distance y_2 from the center of the second jet would be

$$dP_{int} = \text{constant} \left[u^6(y_1) \left| \underline{V}(y_1) - \underline{V}(y_2) \right|^2 + u^6(y_2) \left| \underline{V}(y_1) - \underline{V}(y_2) \right|^2 \right]$$

The total power output from the interaction region is then

$$P_{int} = \text{constant} \int_{\text{volume}} \left(u^6(y_1) + u^6(y_2) \right) \left| V(y_1) - V(y_2) \right|^2 d\tau$$

An approximation to this integral has been obtained by numerical methods, with the use of Lawrence's experimental values for f and g, with $x/r = 5.5$ which corresponds to the distance x that was used in our experiments. This integral has been approximated for several values of the distance between the jet axes, and the result is the calculated curve of Fig. XIV-3. Note that this rough calculation does, indeed, predict two maxima, and the calculated curve has the same general shape as the experimental curve.

U. Ingard, G. C. Maling, Jr.

References

1. Quarterly Report, Acoustics Laboratory, M.I.T., April - June 1957, p. 23.
2. Quarterly Report, Acoustics Laboratory, M.I.T., July - September 1957, p. 18.
3. M. J. Lighthill, On sound generated aerodynamically. I. General theory, Proc. Roy. Soc. (London) A211, 564 (1952).
4. J. C. Lawrence, Intensity, scale and spectra of turbulence in mixing region of free subsonic jet, Report 1292, National Advisory Committee for Aeronautics, Washington, D. C., 1956.

C. FIELD MEASUREMENTS OF SCATTER ATTENUATION OF SOUND IN THE ATMOSPHERE

Of the various factors influencing sound propagation in the atmosphere, the refraction (coherent scattering) of sound by steady temperature and wind gradients, which leads to effects such as shadow zones, is well known (1), but the effects of the random fluctuations in the atmosphere which cause scattering into shadow zones and scatter attenuation are relatively unexplored. Because the sound scattered by turbulence is

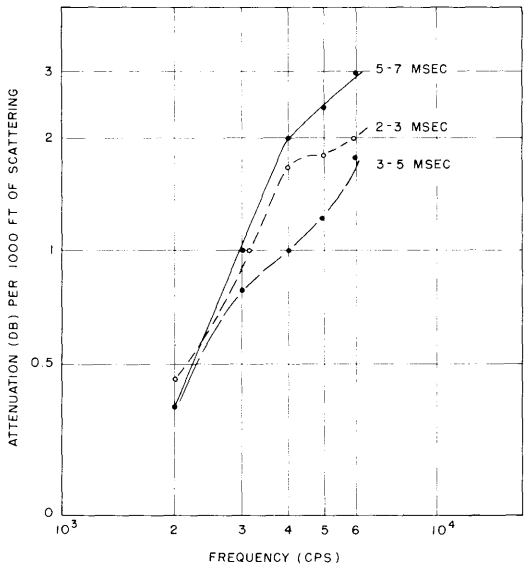

Fig. XIV-4. Example of measured scatter attenuation in the atmosphere.

comparatively small, special precautions have to be taken in experiments that are designed to separate the scatter attenuation from other effects.

Experimental arrangements for measurements of this kind have been described previously in some detail (2). Sound pulses, transmitted from a point on the ground, are followed over a course of approximately 3500 feet by switching (at the speed of sound) over a line of 11 microphones equally spaced over this distance. Measurements were made with pulses at frequencies ranging from 500 cps to 5000 cps. A sufficiently large number of attenuation samples was taken at each frequency, and the averages were evaluated. In the experimental arrangement, the effect of spherical divergence of the wave was compensated for electrically by an individual amplifier for each microphone. Measurements were performed under many different weather conditions. The attenuation with no wind present was found to be in good agreement with the thermal relaxation absorption in the air. The attenuation in excess of this value in the presence of wind was assumed to be caused by scattering. This scattered attenuation was determined in three ranges of mean wind speed: 2-3 $msec^{-1}$, 3-5 $msec^{-1}$, and 5-7 $msec^{-1}$. Results of the scatter attenuation are shown in Fig. XIV-4.

It is interesting to note that the scatter attenuation does not increase monotonically with the increased wind speed. The following discussion is a tentative explanation of this result. Let us assume that the measured attenuation is caused mainly by back scattering, since directivity of the sound field is not very pronounced in this instance. The back scattering is caused mainly by the eddies that are of the order of one wavelength in size. The distribution of the intensity of these eddies, described by the energy spectrum of turbulence, is not independent of the wind speed. Measurements of energy

spectra have shown that, as the wind speed decreases, the intensity of the large eddies decreases approximately as the square of the wind speed, whereas the energy of the smaller eddies remains approximately unchanged, at least when the temperature in the atmosphere decreases with altitude. Consequently, the back scattering, at least for frequencies higher than a certain value, remains approximately unchanged as the wind speed changes. However, since the turbulent spectrum not only changes with the wind speed but also is strongly dependent on the temperature gradient in the atmosphere, much more information is needed about the dependence of the energy spectrum on these variables before quantitative results based on the foregoing argument can be obtained.

U. Ingard, S. K. Oleson

References

1. U. Ingard, The physics of outdoor sound, Proc. Fourth Annual National Noise Abatement Symposium 4, 11 (1953).

2. Quarterly Report, Acoustics Laboratory, M.I.T., January - March 1957, p. 13.

D. SCATTERING OF SOUND BY TURBULENCE

There are two cases of scattering of sound by turbulence which are tractable for theoretical analysis. One concerns the propagation of collimated high-frequency sound beams in a turbulent flow, and the other describes the propagation of a spherically symmetrical wave in a uniform turbulent region. In our studies of scattering of sound by turbulence, the objective is to investigate these two limiting cases in order to gain a better understanding of the mechanism of interaction of sound with turbulence.

A collimated sound beam from a 100-kc electrostatic sound source is propagated through a region of turbulence generated by several small fans. The beam is pulse-modulated, and the pulse has a duration of approximately 1 msec. When no turbulence is present, the received pulse height is, for all practical purposes, constant. In the presence of turbulence, however, there is a distribution in pulse height caused by the scattering of sound in various directions. By studying the pulse-height distribution, it is possible to evaluate the scattered energy.

This method of pulse-height distribution measurement was chosen partly because of the availability of instruments for pulse-height analysis. We are indebted to the Laboratory for Nuclear Sciences, M.I.T., for the loan of a 10-channel pulse-height analyzer. This instrument is designed for pulses with a duration of approximately 1 μsec. The only modification that is needed in our experimental arrangement is the translation of the millisecond acoustic pulses into microsecond pulses. This was accomplished by superposing a constant microsecond pulse upon the envelope of the acoustical pulses, as indicated schematically in Fig. XIV-5. The over-all experimental

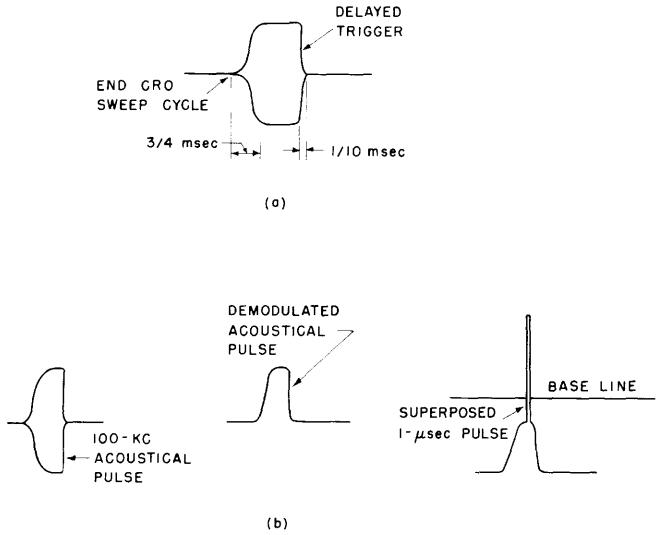

Fig. XIV-5. A constant microsecond pulse is made to "ride" on the demodulated acoustic pulse to enable use of pulse-height analyzer designed for microsecond pulses.

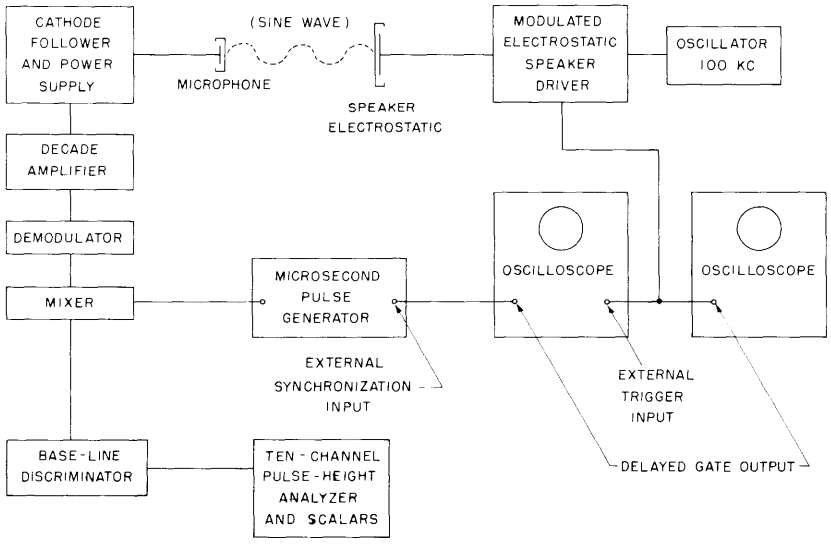

Fig. XIV-6. Block diagram of experimental arrangement for sound-scattering experiment.

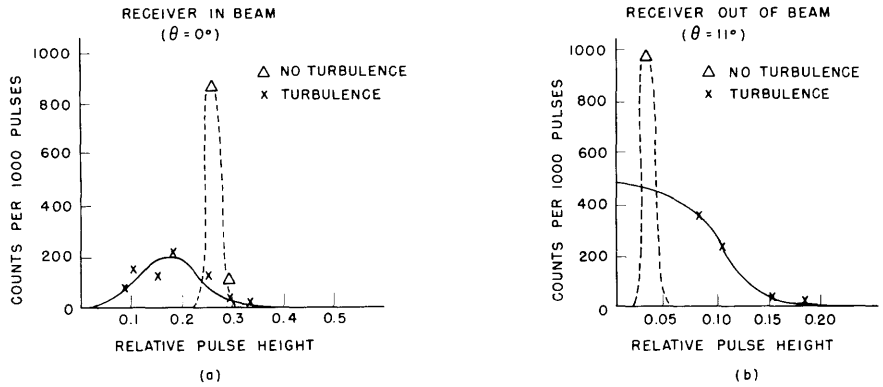

Fig. XIV-7. Examples of measured pulse-height distributions.

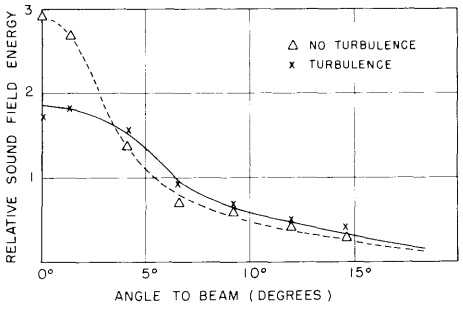

Fig. XIV-8. Intensity distribution in sound beam with and without turbulence.

arrangement is shown in the block diagram of Fig. XIV-6.

With the use of this experimental arrangement, some preliminary measurements have been made. Figure XIV-7a shows the pulse-height distribution both with and without turbulence when the receiver is in the line of the beam behind the turbulent region. Figure XIV-7b shows the corresponding distribution obtained when the receiver is placed outside the beam at a scattering angle of 11°. From such pulse-height distribution measurements, the angular distribution of acoustic intensity with and without turbulence is obtained, as shown in Fig. XIV-8. This figure clearly indicates that energy is scattered out from the beam and causes attenuation of the sound wave. These measurements are, as already mentioned, of a preliminary nature, and a more systematic study along these lines has been started. This study may be extended also to back scattering in a spherical wave.

M. D. Mintz, U. Ingard

E. EXPERIMENTS WITH SPHERICAL ULTRASONIC SOURCES

For certain experiments on the scattering of sound by turbulence, a sound source with spherical symmetry is required. This requirement can be satisfied in several ways.

Our recent experimentation has been based on two different approaches: the first employs the well-known idea of sound generated by a modulated electric discharge; the second involves a modification of an ordinary electrostatic source.

1. Electric-Discharge Ultrasonic Source

A simple modulator that delivers approximately 20 watts to the discharge was designed. The modulator chassis supports a narrow, rigid tripod, terminated in adjustable electrode holders. Various electrode materials and gap configurations were tried in an attempt to obtain the highest acoustic output consistent with spherical symmetry of the sound field and long electrode life. As we expected, the highest output was obtained with the largest gap (approximately 0.5 inch). However, in order to preserve reasonably good spherical symmetry of the radiated sound field, the gap length had to be kept less than approximately 0.15 inch.

To minimize the shadow effect of the electrodes on the radiation field, very fine wire, only a few mils in diameter, was used initially. With materials that have low heat conductivity, such as nichrome, the electrode tips became brilliantly incandescent, and the resultant local heating and ionization increased the acoustic output. However, materials with sufficiently low heat conductivity to attain incandescence soon vaporized, whereas long-lived materials such as platinum did not reach incandescence. Good results were finally obtained by using ceramic-coated filament wires from discarded vacuum tubes.

The nonlinearity of the resistivity of the arc appears to have had a strong demodulating effect, sometimes reducing an 80 per cent modulated carrier to as low as 15 or 20 per cent. Thus, for maximizing the acoustic output, it was necessary to control the linearity of the arc resistance and the power delivered to the gap.

Electrode evaporation caused a slow change in the acoustic power radiated. Moreover, the arc was found to be highly unstable in turbulence. Because of these variations in the acoustic output with time, the electric discharge proved to be unsatisfactory for scattering measurements, but it may be useful in other applications.

2. Electrostatic Ultrasonic Source

In the construction of a spherical electrostatic radiator, the outer radiating shell must be light and stiff to insure a high resonant frequency, and the static capacity between the two electrodes must be reasonably large to provide a satisfactory frequency response. Large capacity requires high field strengths across small gaps, and consequently, dielectric breakdown problems are involved. These problems were overcome in this instance by using a semiconductor (soapstone) for the inner electrode. Polarizing voltages that are considerably higher than those possible with either air or a solid dielectric between metallic electrodes can be applied before breakdown occurs. The spherical

radiator, which consists of a soapstone sphere surrounded by a 1-mil aluminum shell, performs satisfactorily in the audio-frequency region. Its performance at ultrasonic frequencies is being evaluated.

We do not understand completely why the semiconducting sphere works satisfactorily at high polarizing voltages without breakdown and are continuing our study to obtain a more complete understanding of this problem. The effect was first noted by Johnsen and Rahbek (1), in 1917. They demonstrated that a semiconducting foil that was metallized on one side could be made to stick to a metal surface unusually well by the application of a dc potential across the foil.

H. L. Willke, Jr., L. C. Bahiana, U. Ingard

References

1. A. Johnsen and K. Rahbek, A physical phenomenon and its applications to telegraphy, telephony, etc., Jour. Inst. Elect. Engrs. (London) 61, 713 (1923).

F. MEASUREMENT OF THE ATTENUATION OF SOUND IN METAL RODS

An apparatus that is similar to that of Bordoni (1) has been constructed. A cylindrical bar, 1/2 inch in diameter and 2 9/16 inches long, is excited electrostatically at its lowest resonant frequency by means of a flat electrode parallel to one end face. The bar is held by needle points placed in the velocity nodal plane. The capacity between this electrode and the end face varies as the bar vibrates and is an instantaneous measure of the position of the end of the bar. The capacity controls the frequency of an oscillator. The decay of the detected signal from the oscillator gives the decay of sound in the bar. A block diagram of the circuitry is given in Fig. XIV-9.

If the standing wave in the bar decays as $e^{-\delta t}$, the quality factor is given by $Q = \frac{\omega}{2\delta} = 4.34\ \omega\ \frac{\tau}{\Delta}$, where ω is the resonant angular frequency and Δ is the number of

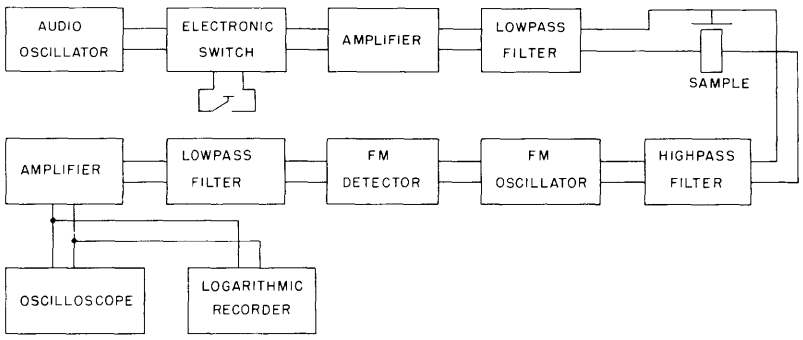

Fig. XIV-9. Apparatus for measuring absorption of sound in metals.

decibels the signal decays in time τ. Measurements have been made on lengths of commercial aluminum rod at room temperature. The observed quality factors range from 1.5×10^{4} to 3.3×10^{4}, which correspond to an attenuation of 1.6×10^{-5} to 0.73×10^{-5} cm^{-1}. These values are in agreement with Bordoni's measurements (1). Scars on the bar such as those made by the needle points seem to decrease the value of Q. A hole 2 mm in diameter drilled through the center perpendicular to the longitudinal axis decreased the value of Q by approximately a factor of 10.

L. W. Dean III

References

1. P. G. Bordoni, Elastic and anelastic behavior of some metals at very low temperatures, J. Acoust. Soc. Am. 26, 495 (1954).

G. AUDIBILITY OF AIRBORNE ULTRASOUND

The ear is usually considered to have no sensitivity at frequencies higher than 20 kcps. A quick survey of the published works does not reveal any attempts to measure threshold levels at any higher frequencies. However, during experiments on the design of ultrasonic sources for air, I could not help but notice that intense high-frequency sound could be heard when the ear was placed in the center of the beam from the radiator. Moving my ear in and out of this beam confirmed this hearing sensation. Although no systematic studies have been made of this effect, since it lies outside the range of our present work, it may be of interest to report briefly on these observations.

As the frequency was increased from 0.2 kcps, my threshold of hearing increased to 117 db (re 0.0002 dyn/cm^2) at 29 kcps. Hearing threshold levels could not be obtained at higher frequencies with the present equipment. However, auditory effects were noted at higher frequencies. These impressions were similar to those obtained when a block of absorbing material (for example, Fiberglas) is placed close to the ear. The impressions lasted several minutes after the source was turned off. Tests of my hearing threshold at 1 kcps and at 15 kcps, before and after a three-minute exposure at 118 db, 37 kcps, showed no change in the sensitivity of the exposed ear.

Modulation effects caused by the nonlinearity of the hearing mechanism were studied in a series of tests which involved a 10-100 cps pulsing of the ultrasonic generator. The pulsing had little subjective effect with a 20-60 kcps carrier but a low disembodied thumping became increasingly audible as the frequency was increased from 60 to 100 kcps. At 100 kcps, the modulated signal was plainly audible even at very low sound pressure levels.

H. L. Willke, Jr.

H. EFFECT OF A PLANE ON THE POWER OUTPUT OF A MONOPOLE

An acoustic monopole can be pictured as a small pulsating sphere whose "strength" for harmonic fluctuations is generally specified by the magnitude of the oscillatory mass flow from the source. This source strength is assumed to be constant in the present analysis. In the presence of an infinite reflecting plane, the effect of the plane is obtained simply by introducing an image source of equal amplitude and phase. However, when the plane is absorbent such an elementary treatment is no longer possible, and the problem then becomes similar to the "Sommerfeld problem" in electromagnetic theory.

The sound energy radiated into the half-space for a constant-strength monopole in the presence of an infinite plane has been investigated, by using existing theory on the reflection of a spherical wave from an infinite plane with boundary conditions specified by an acoustic admittance (1). If we denote the power output of the source in free space by W_o, and the power radiated into half-space in the presence of the boundary by W_{rad}, it can be shown that, when the boundary admittance is purely real and equal to β, the ratio W_{rad}/W_o is expressed as

$$\frac{W_{rad}}{W_o} = \frac{1+3\beta}{1+\beta} + 2\beta \log_e \frac{\beta}{1+\beta} + \frac{\sin z}{z}$$

$$- 2\beta\left[\cos z\beta(\mathrm{Ci}(z\beta + z) - \mathrm{Ci}(z\beta)) + \sin z\beta(\mathrm{Si}(z\beta + z) - \mathrm{Si}(z\beta))\right] \qquad (1)$$

where Si(x) and Ci(x) are sine and cosine integrals, respectively; $z = 2kh$, where h is the height of the source above ground; and $k = \omega/c$. Figure XIV-10 shows W_{rad}/W_o for $\beta = 0$, 1 and ∞ as a function of z. For a source in the plane ($z \to 0$) or for a source high above the plane ($z \to \infty$), Eq. 1 reduces to

$$\frac{W_{rad}}{W_o} = \frac{2(1+2\beta)}{1+\beta} + 4\beta \log \frac{\beta}{1+\beta} \qquad (z \to 0) \qquad (2)$$

$$\frac{W_{rad}}{W_o} = \frac{1+3\beta}{1+\beta} + 2\beta \log \frac{\beta}{1+\beta} \qquad (z \to \infty) \qquad (3)$$

These expressions have been plotted in Figs. XIV-11 and XIV-12.

The effect of a plane on the total power output (W) of the sound source was investigated in a previous report (2). Additional curves for W/W_o as a function of z have been plotted, and are shown in Fig. XIV-13. Clearly, the difference between the power radiated by the source (W) and the power radiated into the hemisphere (W_{rad}) must be the power absorbed by the boundary so that the boundary absorption can be easily evaluated by this method.

G. C. Maling, Jr.

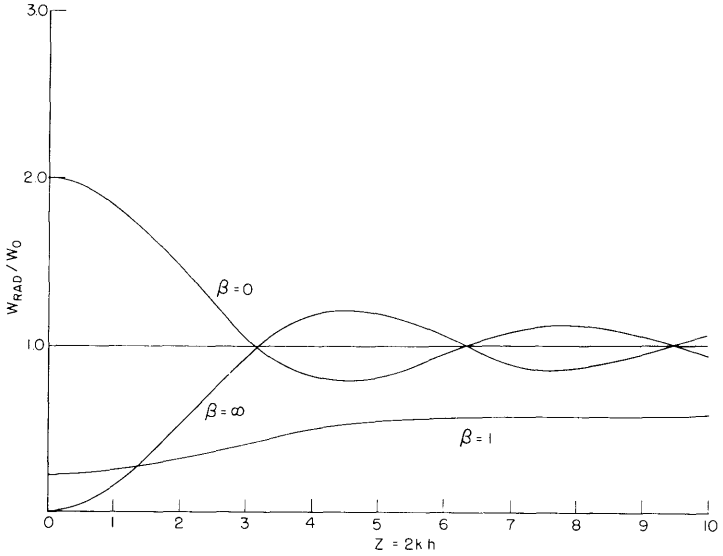

Fig. XIV-10. W_{rad}/W_o as a function of z.

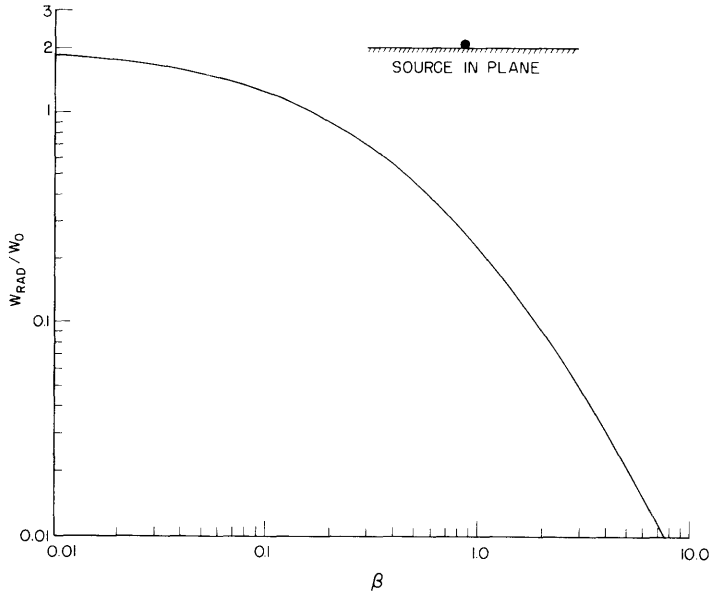

Fig. XIV-11. W_{rad}/W_o as a function of β ($z \to 0$).

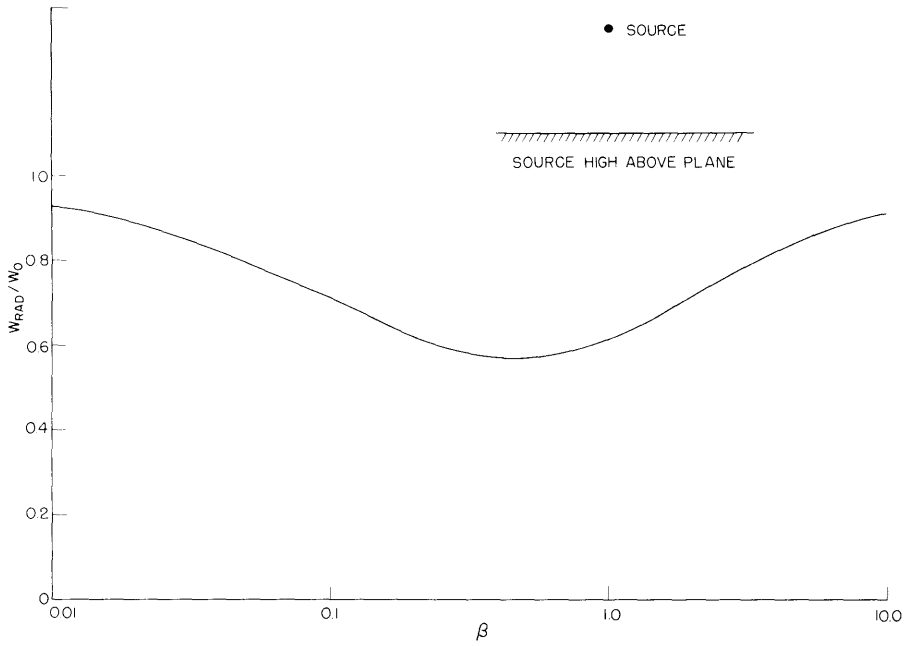

Fig. XIV-12. W_{rad}/W_o as a function of β ($z \to \infty$).

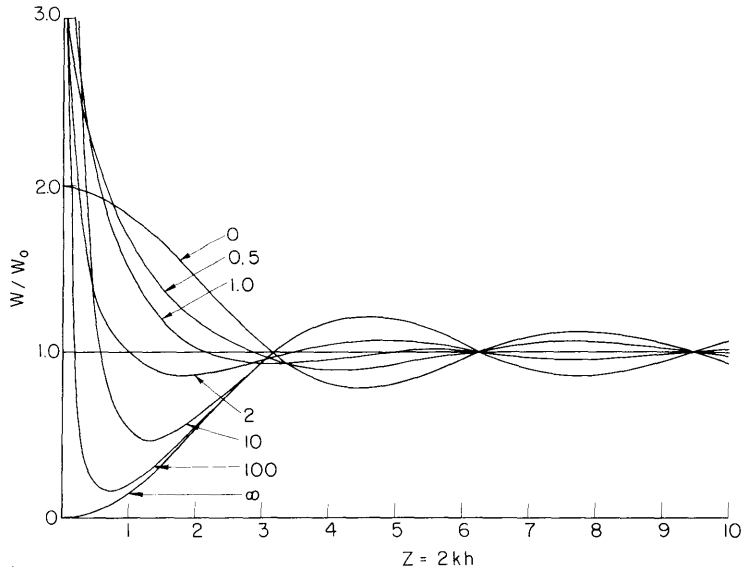

Fig. XIV-13. W_{rad}/W_o as a function of z.

References

1. U. Ingard, On the reflection of a spherical sound wave from an infinite plane, J. Acoust. Soc. Am. 23, 329 (1951).

2. Quarterly Report, Acoustics Laboratory, M.I.T., July-September 1957, p. 15.

I. THE ACOUSTIC IMPEDANCE OF A FLEXIBLE, POROUS MATERIAL

It is well known that the acoustic properties of a homogeneous, porous substance depend upon its flow resistance, porosity, and structure factor (1). Many investigators have studied the behavior of such a material when it is used as a layer in front of a hard wall (2). Morse (3) has given an equivalent electrical circuit for a porous tile backed by a hard wall from which its acoustic impedance and the percentage of incident sound energy that is absorbed can be determined. In many engineering materials, the skeleton is not rigid and wave motion will propagate in the structure as well as in the pores. A general analysis of this problem is complicated by the coupling between these wave motions (4). However, much useful information on the performance of a nonrigid porous tile can be obtained from a simple equivalent circuit. The electrical analog of Fig. XIV-14 is similar to that given by Morse (3), except that a second branch has been added in parallel to account for the wave motion in the structure itself. The elements of this branch correspond to the mass, compliance, and viscous resistance of the flexible structure.

In Fig. XIV-15 the impedance calculated from the equivalent circuit of Fig. XIV-14 is compared with measured values of the impedance for a typical porous material with a flexible structure. The performance of the material is fairly well predicted by the

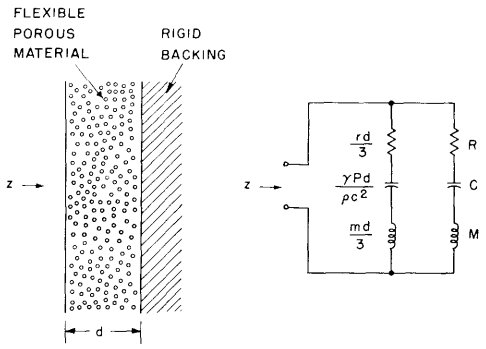

Fig. XIV-14. Rigid-backed, flexible, porous tile and equivalent circuit.

r = specific flow resistance
P = porosity
d = thickness
m = effective mass of air in pores
C = compliance of structure
M = mass of structure
R = internal resistance of structure

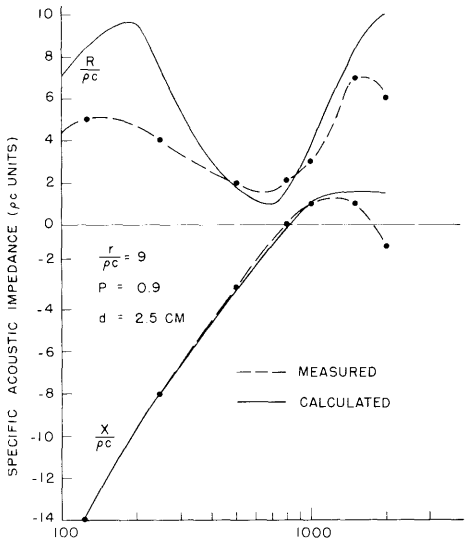

Fig. XIV-15. Measured and calculated impedance for typical flexible, porous tile.

equivalent circuit. The discrepancies can be partly accounted for by the fact that there is no coupling between the two branches of the equivalent circuit, whereas for all flexible, porous media there will be coupling between the structure-borne and air-borne waves.

W. W. Lang

References

1. C. Zwikker and C. W. Kosten, Sound Absorbing Materials (Elsevier Publishing Company, New York, 1949), p. 20.

2. P. M. Morse and R. H. Bolt, Sound waves in rooms, Revs. Modern Phys. 16, 95 (1944).

3. P. M. Morse, Vibration and Sound (McGraw-Hill Book Company, New York, 2d edition, 1948), p. 365.

4. W. W. Lang, Sound propagation in flexible, porous media, J. Acoust. Soc. Am. 30, 670 (1958).